

RESEARCH ARTICLE

Analysis of the Biological Function of ELDF15 Using an Antisense Recombinant Expression Vector

Yan Liu¹, Long Wang², Zi-Jun Wang^{1*}

Abstract

ELDF15, homologous with AT2 receptor-interaction protein 1 (ATIP1), may play an important role in cell differentiation, proliferation, and carcinogenesis. We aimed to understand the biological function of ELDF15 via construction and transfection of a recombinant expression vector containing antisense ELDF15. Recombinant expression vectors were successfully constructed and transfected into K562 cells. A stable transfectant, known as pXJ41-asELDF15, stably produced antisense ELDF15. Compared with K562 and K562-zeo cells, K562-pXJ41-asELDF15 cells showed inhibition of cell proliferation. RT-PCR analysis showed that the expression and protein level of ELDF15 decreased significantly in K562 cells transfected with pXJ41-asELDF15. Expression of hemoglobin increased in K562 cells transfected with pXJ41-asELDF15 by benzidine staining. Increases in NBT reduction activity in K562 cells transfected with pXJ41-asELDF15. Colony forming efficiency in two-layer soft agar was clearly inhibited as assessed by electron microscopy. These results suggest that ELDF15 plays a potential role in cell differentiation, proliferation and carcinogenesis.

Keywords: ELDF15 - gene - cell proliferation - differentiation - antisense technology - carcinogenesis

Asian Pac J Cancer Prev, 15 (21), 9131-9136

Introduction

The development and differentiation of human cells are complex processes controlled by a series of genes. The key to normal cell differentiation is the orderly expression of key genes at the appropriate time and in the correct location. Under normal circumstances, these genes are activated and inhibited selectively according to a sequence of tightly controlled events. If genes that influence cellular development are expressed out of order, abnormal differentiation and carcinogenesis may result. Carcinogenesis takes place over a long period of time. There are several phases to carcinogenesis, as well as mutations in many genes (Horiuchi et al., 2012). Approximately 100 oncogenes and 10 tumor suppressor genes have been documented to date, but there are still many unknown genes that influence cell development (Chen and Pan, 2006; Cao, 2012). Therefore, to better understand the process of carcinogenesis, we must first characterize the ways in which cancer is induced.

ELDF15, known as embryonic liver cell differentiation factor (ELDF15, GenBank accession number AF394227), is located on chromosome 8p21.3-p22 and the length of the entire gene was found to be 1970 bp (Liu et al., 2003). The Homo sapiens AT2 receptor-interaction protein 1 (ATIP1) has the highest degree of homology with ELDF15, at 100% homology (Olin et al., 2011). Previous research indicated

that this gene shows high expression in less differentiated embryonic tissues, cancer tissues and human cell lines. ELDF15 expression in normal differentiated mature cells and tissues around tumors was obviously decreased. This finding suggests that ELDF15 gene may play an important role in cell differentiation, proliferation, and carcinogenesis. In the present study, to better understand the function of ELDF15, we transfected K562 cells with an antisense recombinant ELDF15 expression vector and studied the effects of ELDF15 inhibition.

Materials and Methods

Construction of recombinant eukaryotic expression vector

The 130-bp DNA fragment was amplified from ELDF15 cDNA open reading frame (ORF) with the primers (forward) 5'- GACTCGAG ATG TTG TCG TCT CCC AAA TTC TC-3' and (reverse) 5'- GC GGATCC TCG AGG ATT CTT TTG CCT GC-3', which contain restriction digest sites for XhoI and BamHI, respectively. PCR conditions were as follows: initial denaturation at 94°C for 5 min, 30 cycles of 94°C for 30 s, 54°C for 30 s and 72°C for 40 s, and a final extension at 72°C for 5 min. The eukaryotic expression vector pXJ41-neo and the 130-bp PCR product were digested with BamHI and XhoI, and the resulting products were ligated with DNA Ligation Kit (Mighty Mix), and transformed into DH5 α

¹Chinese Center for Disease Control and Prevention, ²Beijing Laboratory Animal Research Center, Beijing, China *For correspondence: longwang888666@aliyun.com

cells. Extracted plasmids were analyzed by the restrictive endonuclease digestion and sequence analysis (Niu et al., 2012). The final recombinant plasmid vector was designated as pXJ41- asELDF15.

Cell culture

Human leukemia K562 cells, obtained from the American Type Culture Collection were maintained as suspension cultures in Dulbecco's modified Eagle medium (DMEM; Gibco, USA) supplemented with 10% (v/v) heat-inactivated fetal bovine serum (FBS), 100 U/mL penicillin, and 100 µg/mL streptomycin at 37°C with 5% humidified CO₂ (Li et al., 2012).

Transfection

Transfections were performed using Lipofectamine 2000 according to the manufacturer's instructions (Huang et al., 2011). Briefly, K562 cells were seeded in six-well plates at a density of 4×10⁵ cells per well in DMEM without antibiotics. The following day, when cultures were 30%-50% confluent, the medium was changed to 1.5 mL Opti-MEM Reduced Serum Medium (Gibco, USA) 1 h before transfection. Five microliters of Lipofectamine 2000 (Invitrogen, USA) was added to 250 µL Opti-MEM Reduced Serum Medium, mixed gently, and incubated at room temperature for 5 min. In parallel, 5, 8 and 12 µL pXJ41-asELDF15 (20 µM) was added to each aliquot of 250 µL Opti-MEM Reduced Serum Medium, mixed with the diluted oligomer and Lipofectamine 2000, and incubated at room temperature for 20 min before addition to the cells at a final concentration of 50, 80 and 120 nM, and cotransfected into K562 cells. The transfected cells were cultured at 37°C with 5% CO₂. The transfection medium was replaced with fresh medium supplemented 10% FBS 4-6 h post-transfection and fed daily with fresh medium. A blank control group (K562 cells without treatment) and a negative control group (K562 cells transfected with pXJ41) were concurrently established.

Total RNA extraction and cDNA synthesis

Total RNA was extracted using TRI Reagent (Sigma Aldrich, USA) according to the manufacturer's protocol. RNA was diluted in 20 µL of RNase-free water, quantified by spectrophotometry at 260 nm and stored at -20°C. RNA with a 260/280 nm ratio in the range of 1.8-2.0 was considered high quality. First-strand cDNA was synthesized from each RNA pool using PCR Kit ver. 3.0 (Takara Bio Inc., Japan) according to the manufacturer's instructions. Briefly, 1 µg of RNA was combined with 2.5 pM of oligo dT-adapter primer, 4 µL of 25 mM MgCl₂, 2 µL of 10× RNA PCR buffer, 2 µL of 10 mM dNTP mixture, 20 units of RNase inhibitor, 5 units of AMV Reverse Transcriptase XL, and RNase-free water to a total volume of 20 µL. The reaction took place at 42°C for 30 min, followed by 95°C for 5 min and 5°C for 5 min in a GeneAmp PCR System 9700 (Perkin-Elmer Co, USA). The resulting cDNA was stored at -20°C.

Real-time quantitative PCR (qRT-PCR)

Forty-eight hours after transfection, the K562 cells were collected and the total RNA was extracted. Two

micrograms of total RNA was reverse transcribed to synthesize single-stranded cDNA (ss-cDNA) products as described above. A standard 20µL reaction contained 0.5µL of the cDNA mixture, 0.25µL of the forward and reverse primers (100 µM stock) and the SYBR Green Master Mix. Amplification was performed for 40 cycles under the following PCR conditions: 1 minute at 95°C, 1 minute at 60°C and 1 minute at 72°C. Samples were run in triplicate in a 96-well plate format in a 7500 Real-Time PCR System. The ELDF15 primers were: (forward) 5'-GA CTCGAG ATG TTG TTG TCT CCC AAA TTC TC-3' and (reverse) 5'-GC GGATCC TCG AGG ATT CTT TTG CCT GC-3'. Glyceraldehyde 3-phosphate dehydrogenase (GAPDH) primers were also used with total RNA purified from cells transfected with our recombinant vector as control. The primers were (forward) 5' - CCA TCA CCA TCT TCC AGG AG -3' and (reverse) 5' - CCT GCT TCA CCA CCT TCT TG -3'. The reactions were performed in duplicate. The amount of mRNA in our samples was quantified by the ΔCt method.

Cell growth curve and proliferation inhibition analysis

K562 cell growth was measured using MTT [3- (4,5-dimethylthiazol-2-yl)-2,5-diphenyl tetrazoliumbromide] assays. Single cell suspensions were prepared in DMEM supplemented with 10% FBS, and seeded in 96-well plates at a density of 5×10³ cells per well in 200 µL medium. Cells were seeded in triplicate for each group and were transfected with 120 nM pXJ41- asELDF15, pXJ41 and blank control. At the end of each incubation period, 20 µL MTT (0.5 mg/mL; Amresco, USA) was added, and cells were incubated for 0d,1d,2d,3d,4d, or 5d under standard cell culture conditions. The medium was then removed, and 200 µL DMSO (Amresco, USA) was added to each well. Absorbance was measured with an ELISA plate reader at 570 nm. The presented values represent the means of triplicate wells from which cell growth curves and proliferation inhibition ratios were determined (Gao et al., 2012).

Flow cytometric analysis for cell cycle

(1) PI staining: Cells were collected after treatment and washed 3 times with PBS, incubated with PBS containing 100 µg/mL propidium iodide (PI), 1% Triton X-100, 100 U/mL RNase for 30 min at 37°C, followed by FACS analysis.

(2) Annexin V FITC labeling: phosphatidylserine (PS) expression on the external surface of cells was detected using binding to FITC-labeled annexin V. Cells were collected and washed once with cold PBS and centrifuged to collect the cell pellet which was then resuspended in cold binding buffer (10 mM HEPES/NaOH, pH 7.4, 140 mM NaCl, 5 mM CaCl₂). Annexin V-FITC (final concentration 1 µg/mL) was added and mixed gently. The tubes were then incubated for 15-20 min in the dark prior to flow cytometry (Wang et al., 2009).

Immunocytochemistry

pXJ41-ELDF15 and pXJ41 were detected using immunofluorescent staining. Immediately after the sham

or RF field exposure, cells were washed with cold PBS, and fixed with 3.7% formaldehyde. Cell membranes were permeabilized with 0.25% Triton X-100 in PBS at room temperature. Non-specific binding sites were blocked with 1% bovine serum albumin (BSA) in PBS for 30 min. Cells were incubated with anti-goat polyclonal antibody (1:100, C-20 Santa Cruz Biotechnology) or anti-pXJ41 rabbit polyclonal antibody (Stressgene) for 1 h, washed, incubated with FITC-conjugated anti-goat or anti-rabbit IgG (1:100, Santa Cruz Biotechnology), and examined under an Olympus fluorescence microscope (Ding et al., 2009).

Photos were taken using a mounted digital camera. Fluorescent cells were counted in five different microscope areas, and the percentage of positive cells was calculated by dividing the number of fluorescent cells by the total number of cells in these five areas.

Benzidine staining

Benzidine dihydrochloride (Sigma, USA) staining to identify hemoglobin-containing cells was carried out according to the Palis method, with slight modifications. Briefly, 20 μ L of 30% hydrogen peroxide was added to 1 mL of benzidine immediately before use. A 200 μ L aliquot of the resulting solution was added to the cells, which were then examined using an inverted microscope. Benzidine-positive cells stained dark blue as a result of the reaction between hemoglobin and H₂O₂, while benzidine-negative cells were light yellow (Mohammad et al., 2009).

Nitroblue tetrazolium reduction test

The degree of differentiation was assayed by the ability of the cells to reduce nitroblue tetrazolium (NBT) into insoluble blue-black formazan upon stimulation with PKC activator (PMA). Each cell suspension (100 μ L) was mixed with an equal volume of 2 mg/mL NBT dissolved in PBS containing 1 μ g/mL PMA and incubated at 37°C for 30 min. The reaction was halted with the addition of 0.4 mL cold 2 M HCl. The formazan product was obtained by centrifugation of the sample at 700 \times g for 10 min. The supernatant was discarded, and the formazan was dissolved in 600 μ L DMSO. The percentage of NBT-positive cells with formazan deposits in the cytoplasm was determined by spectrophotometry at 572 nm (Sanjeev et al., 2013). The data are expressed as a percentage of the control value.

Colony formation in soft agar

A two-layer soft agar system was prepared in 30 mm wells (3~661 Castor, Cambridge Mass.). Briefly, the lower agar layer in each well had a total volume of 2.5 mL and was composed of 1.25 mL RPMI 1640, 0.375 mL 2 \times RPMI 1640, 0.5 mL heat-inactivated FCS, 0.375 mL of a stock 3.3% agar solution, and PHA-M, PWM (1 μ L/mL), protein A, or supernatant factors from human peripheral blood cells stimulated with PHA or PWM. This layer, which had a final agar concentration of 0.5%, was prepared and allowed to equilibrate at 37°C in air containing 5% CO₂ for 4-24 h before use. The upper agar layer had a total volume of 0.85 mL composed of 0.3 mL 2 \times RPMI 1640, 0.15 mL distilled water, 0.15 mL FCS, 0.15 mL of

a 1.8% agar solution, and 0.1 mL RPMI 1640 containing 1 \times 10⁶ cells from the initial suspension culture. The final agar concentration in the upper layer was 0.32%. The culture dishes were incubated at 37°C in a humidified atmosphere containing 5% CO₂. Colony development was observed through an inverted microscope. The number of colonies was determined at 4-6 days after seeding by counting colonies of 50 or more cells from six culture plates for each experiment (Liu et al., 2013).

Electron microscopy

The group with high percent of transfected K562 cells colonies was selected for transmission electron microscopy (TEM) evaluation. According to our statistical analysis, the colonies were collected from the semisolid serum free media group containing 20 ng/mL BMP-4, fixed in 2.5% glutaraldehyde in PBS (pH 7.4) for 2 h, and post-fixed with 1% osmium tetroxide in the same buffer for 2 h. After dehydration in a graded ethanol series, the cells were placed in propylene oxide and embedded in Epon 812. Semi-thin sections (0.5 μ m) were stained with toluidine blue for light microscopy. Ultra-thin sections were stained with uranyl acetate and lead citrate and examined by TEM (Zeiss EM 900) (Mohammad et al., 2009).

Statistical analyses

All experiments were repeated three times and statistical analyses were performed using SPSS 10.0. *P* values of <0.05 were considered to be statistically significant.

Results

Amplification of ELDF15 and construction of the pXJ41-asELDF15 plasmid

PCR products were electrophoresed on a 2% agarose gel. The length of the observed product was approximately 130 bp, consistent with the expected size of ELDF15 (Figure 1A). The recombinant pXJ41-asELDF15 plasmid was verified by restriction endonuclease analysis and DNA sequence analysis (Figure 1B). The sequencing results show that the ELDF15 sequence in the plasmid is identical to the ELDF15 sequence recently reported on PubMed. We concluded that the recombinant plasmid vectors pXJ41-asELDF15 were constructed successfully.

pXJ41-asELDF15 inhibits ELDF15 mRNA expression

Forty-eight hours after transfection, the cells were collected and the expression of ELDF15 was detected by qRT-PCR, which demonstrated the expression of ELDF15 mRNA was decreased in cells transfected with the pXJ41-asELDF15 plasmid, when compared to the two control groups (Figure 1C).

pXJ41-asELDF15 inhibits K562 cell proliferation

K562 cells were transfected with pXJ41-asELDF15 in 96-well plates, and cell proliferation was assessed by MTT assays. Cell proliferation in the negative control transfected and the K562 blank control groups was similarly unaffected, but the proliferation of transfected pXJ41-asELDF15 cells was inhibited (Figure 2A).

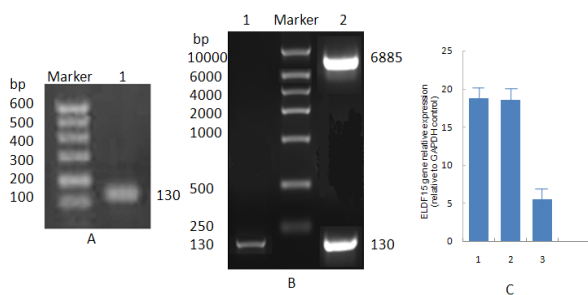


Figure 1. A) Agarose Gel of PCR Product. M: DNA marker DL600; Lane 1: PCR product using ELDF15 primers; **B) Restrictive Endonuclease Digestion of Recombinant Plamid pXJ41-asELDF15;** M: DNA marker DL10000; Lane 1: ELDF15 PCR product. Lane 2: Product of recombinant plasmid pXJ41-asELDF15 by restriction digest; **C) Expression of ELDF15 mRNA was Detected by Real-time PCR.** 1. Transfected blank control group. 2. Transfected negative control group. 3. K562 cells were transfected with pXJ41-asELDF15. GAPDH mRNA expression levels were used as the endogenous reference. Gene expression levels were normalized to GAPDH and presented as fold change ($2^{-\Delta\Delta C_t}$) above control group. The data are expressed as mean \pm SD from three independent experiments with three replicates per experiment

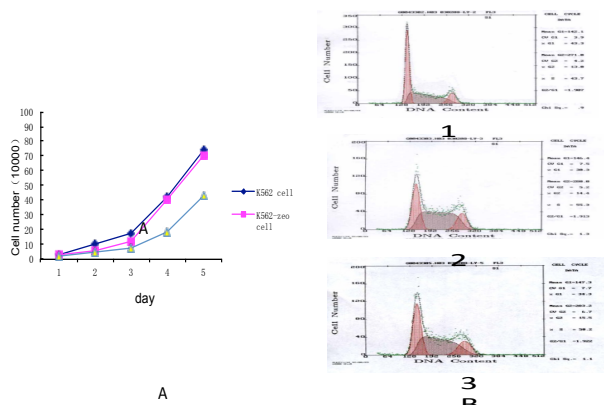


Figure 2. A) asELDF15 Inhibits Cell Proliferation in K562 Cells. MTT assay was used to examine the relative proliferation rate of K562 cells after transfection with pXJ41-asELDF15 for 1, 2, 3, 4 and 5 days. During prolonged transfection with pXJ41-asELDF15, the cell proliferation rate gradually decreased. The difference between each group is statistically significant (* $p < 0.05$, ** $p < 0.01$ compared with control). **B) Effect on Cell Cycle by FACS with PI Staining.** 1. K562 cells transfected with pXJ41-asELDF15. 2. K562 cells transfected with pXJ41. 3. K562 cells without treatment. Values are presented as mean \pm SEM of three assays performed independently

PXJ41-asELDF15 leads to increased cell cycle arrest in G1 phase

FCM was performed to investigate the effect of asELDF15 expression on cell cycle progression in K562 cells after transfection. The results show that asELDF15 expression leads to the arrest of K562 cells at the G1 phase and a decrease in the number of cells in S phase when compared with the control groups. The cell cycle distribution of transfected with pXJ41-asELDF15 cells was analyzed by flow cytometry. Cells were transfected for 48h before processing and analysis. Our results indicate that cells transfected with pXJ41-asELDF15 had increased

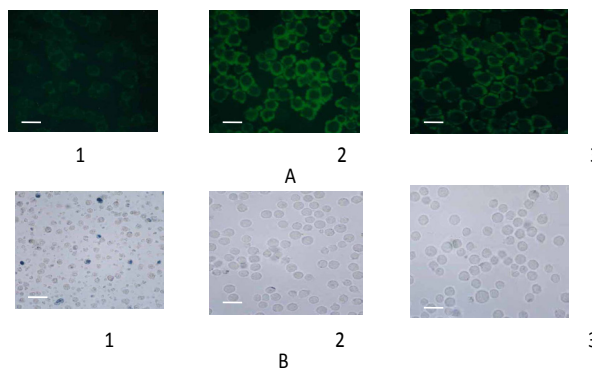


Figure 3A. Protein Expression by Immunohistochemical Analysis. 1.Expression of ELDF15 protein in K562 cells transfected with pXJ41-asELDF15. 2. K562 cells without treatment. 3. K562 cells transfected with pXJ41. Bar=30 μ m. **Figure. 3B. Expression of Hemoglobin by Benzidine Staining.** 1. K562 cells transfected with pXJ41-asELDF15. 2. K562 cells transfected with pXJ41. 3. K562 cells without treatment. The benzidine positive colonies formed after transfection with pXJ41-asELDF15. Bar=20 μ m

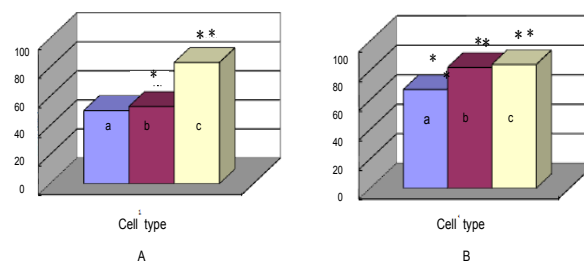


Figure 4. NBT Test to Assay Reductive Activity in K562 Cells. A) K562 cells transfected with pXJ41. B) untransfected K562 cells. C) K562 cells transfected with pXJ41-asELDF15. The cells transfected with pXJ41-asELDF15, pXJ41, and untransfected K562 cells showed an NBT reductive rate of 83.4%, 50.3% and 53.1%, respectively. * $p < 0.05$, ** $p < 0.01$ compared to the control group. **Figure 4B. Inducing asELDF15 Expression in K562 Cells Reduced Cell Proliferation and Colony Formation.** A) K562 cells transfected with pXJ41-asELDF15. B) K562 cells transfected with pXJ41. C) untreated K562 cells. The numbers of colonies were 67%, 82%, and 84%, respectively.* $p < 0.05$, ** $p < 0.01$ compared to the control group

cell populations in the G1/G0 phase with a simultaneous reduction in the number of cells in the S phase. Therefore, we conclude that asELDF15 inhibits cell proliferation (Figure 2B).

Expression of asELDF15 leads to decreased ELDF15 protein expression

ELDF15 is primarily located on the membrane of K562 cells. Of the cells we analyzed, K562 cells transfected with pXJ41-asELDF15 exhibited low levels of ELDF15 protein and weak immunofluorescence. The control groups show strong immunofluorescence (green) when incubated with antibodies against ELDF15. Therefore, we conclude that the expression of ELDF15 protein in K562 cells transfected with pXJ41-asELDF15 is decreased (Figure 3A).

Expression of hemoglobin

Cells were benzidine positive and dark blue when

transfected with pXJ41-asELDF15 (Figure 3B), while K562 cells transfected with pXJ41 were benzidine-negative and light yellow. Therefore, hemoglobin expression increased when K562 cells were transfected with pXJ41-asELDF15. It demonstrated that ELDF15 promotes K562 cell differentiation.

Increased NBT reductive activity in pXJ41-asELDF15-transfected K562 cells

The degree of induced cell differentiation was detected by the Nitroblue Tetrazolium (NBT) reduction test. An increase in the cells' ability to reduce NBT signifies that the cells are fully differentiated. The pXJ41-asELDF15-transfected cells showed an NBT reduction rate of 83.4%, while the pXJ41-transfected and untransfected K562 cells showed an NBT reduction rate of 50.3%, and 53.1%, respectively. These findings suggest that ELDF15 can induce K562 cell differentiation (Figure 4A).

Cell-colony suppression in the rransfected K562 cells

Using our colony formation assay, the number of colonies in the pXJ41-asELDF15-transfected cells decreased greatly (Figure 4B) compared to the untransfected control K562 and K562-zeo cells. The numbers of colonies were 67%, 82% and 84%. The colony sizes in the pXJ41-asELDF15-transfected cells were smaller than the other groups. These findings show that transfection with pXJ41-asELDF15 can suppress cell colony formation.

Ultrastructure of morphological changes of colony cells

Cells transfected with pXJ41-asELDF15 showed altered morphology under the electron microscope. The volumes of cells were small. The chromatin was rough and concentrated. Their numbers of nucleoli was reduced. The shape of the nucleus was irregular and kidney shaped when compared to the negative control colony cells (Figure 5A, B).

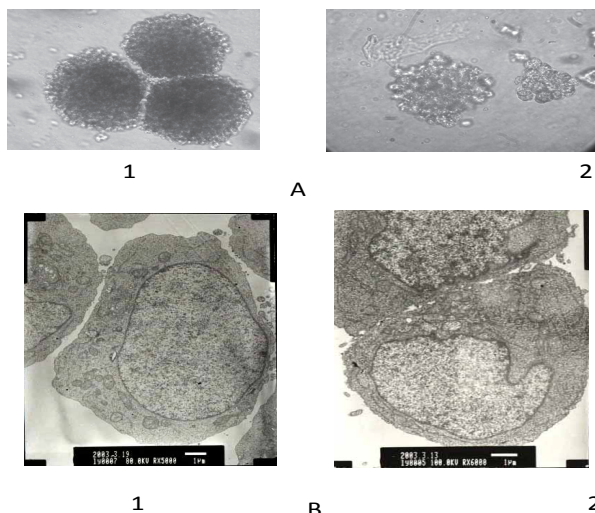


Figure 5A, 5B. Changes in Cell Colony Morphologies.

1. K562 cells transfected with pXJ41. 2. K562 cells transfected with pXJ41-asELDF15. Semi-thin section of K562 colony transfected with pXJ41-asELDF15 under light microscopy showing the reduced cell volumes. Electron micrograph of K562 colony transfected with pXJ41-asELDF15 showing rough and dense chromatin and reduced number of nucleoli. 3100X magnification

Discussion

Cell differentiation is very complex process and the synthesis of specific proteins at the correct times is critical during the process. A simplified mechanism of cell differentiation relies on the expression of a number of proteins that regulate the expression of tissue-specific genes. Eventually, these specific proteins, expressed differently in time and space, define each cell type and specialize cells for different functions.

Tumor cells are the results of aberrant cell differentiation and errors that accumulated during the differentiation process. Oncogenes are tumor-inducing genes that result from mutations of genes that normally code for proteins that help regulate cell growth and differentiation. Usually, anti-oncogenes code for proteins that can prevent cell cycle progress at the cell cycle checkpoints and turn off cell growth. Once inactivated, anti-oncogenes lose their negative regulatory ability, which eventually leads to excessive cell proliferation, ultimately inducing tumorigenesis (Pappou and Ahuja, 2010; Pylayeva et al., 2011).

The activation of oncogenes and inactivation of anti-oncogenes play critical roles in tumorigenesis (Wei et al., 2012; Dean and Knudsen, 2013; Taylor et al., 2013; Wang et al., 2013). These proteins regulate signaling pathways involved in cell cycle progression, apoptosis (Sleena et al., 2012), chromosomal stability, cell differentiation, and morphological changes. It has been reported that activation of oncogenes occurs widely in human tumors (Guo et al., 2014) and inhibition of oncogene expression has obvious effect on cancer therapy. Oncostatin M (OSM) is a multifunctional cellular regulator acting on a wide variety of cells, which has potential roles in the regulation of gene activation, cell survival, proliferation and differentiation. Previous studies have shown that OSM can induce morphological and/or functional differentiation and maturation of many tumor cells. Their findings indicated that OSM could induce the differentiation and reduce cell viability of SMMC-7721 cells, suggesting that differentiation therapy with OSM offers the opportunity for therapeutic intervention in HCC (Kong et al., 2013). Src homology 2 domain containing (SHC) is a proto-oncogene which mediates cell proliferation and carcinogenesis in human carcinomas. The findings indicated that SHCBP1 may contribute to human hepatocellular carcinoma by promoting cell proliferation and may serve as a molecular target of cancer therapy (Tao et al., 2013). The mechanisms behind oncogene activation are possibly viral integration, gene translocation, proto-oncogene amplification and point mutations.

How can the expression of a gene be promoted during the embryonic period and suppressed during the adult stage? Why is the low protein expression level during the adult stage increased in carcinogenesis? Hitherto, there have been no clear explanations for those unconventional regulatory mechanisms. The fact that both tumor and early embryonic tissue have partial common antigenicity and immunity hints at the probability that embryonic genes are expressed in tumors. The ELDF15 gene follows the pathological pattern described above. It is expressed

during the embryonic period and transcription of the gene is turned off in adult cells. Once a tumor forms, transcription of the gene is turned back on and protein expression is increased. This approach may represent a typical model in eukaryotic cells and our experiments may be helpful in deciphering the mechanism behind the reactivation of embryonic genes in tumor cells.

It was reported that ELDF15 is a human AT2 receptor-interacting protein 1 (ATIP1) and primarily located on the membrane of K562 cells. How can cell differentiation be regulated from the cell membrane to the cell nucleus? The mechanism should be further researched.

In our study, the pXJ41-asELDF15 recombinant vector was successfully constructed and transfected into K562 cells. We found the transfected cells lowered their expression of ELDF15 at the mRNA and protein levels. K562 cell proliferation was assessed by MTT assays, which showed that K562 proliferation was inhibited when the cells were transfected with pXJ41-asELDF15. The results of FCM analysis showed that the expression of antisense ELDF15 arrested K562 cells in the G1 phase and resulted in a decrease of cells in the S phase, indicating that cell proliferation was inhibited. Measuring hemoglobin expression using benzidine staining showed that hemoglobin expression increased in K562 cells transfected with pXJ41-asELDF15. It demonstrated that ELDF15 promotes K562 cell differentiation.

We have also shown that the expression of asELDF15 results in increased cell differentiation using an NBT reduction assay. Our results also showed that the total number of colony cells were lower when cells were transfected with pXJ41-asELDF15, and the colonies were smaller. Under TEM, the features of the cells transfected with pXJ41-asELDF15 were significantly changed compared to wild-type.

Based on the above discussion, we believe that an antisense version of the ELDF15 gene can induce cell differentiation through repression of ELDF15 expression. Therefore, in summary, this study demonstrated that antisense ELDF15 significantly promotes cell differentiation. These results suggest that ELDF15 plays a role in cell differentiation, proliferation and carcinogenesis and provides us with a new target for researching the mechanism of carcinogenesis and targeting gene treatment.

References

- Ali Owchi M, Salehnia M, Moghadam MF, Boroujeni MB, Hajizadeh E (2009). The effect of bone morphogenetic protein 4 on the differentiation of mouse embryonic stem cell to erythroid lineage in serum free and serum supplemented media. *Int J Biomed Sci*, **5**, 275-82.
- Chen WC, Pan SL (2006). Recent advancement of tumor suppressor genes and their association with cellular senescence. *Med Recap*, **12**, 711-13.
- Cao YL (2012). Research progress of cancer genes and their detection methods. *Life Sci Instr*, **10**, 10-6
- Dean JL, Knudsen KE (2013). The role of tumor suppressor dysregulation in prostate cancer progression. *Curr Drug Targets*, **14**, 460-71.
- Ding GR, Wang XW, Li KC, et al (2009). Comparison of Hsps expression after radio-frequency field exposure in three human glioma cell lines. *Biomed Environ Sci*, **22**, 374-80.
- Gao HX, Gao XF, Wang GQ, et al (2012). In vitro study of nucleostemin gene as a potential therapeutic target for human lung carcinoma. *Biomed Environ Sci*, **25**, 91-97.
- Guo XE, Ngo B, Modrek AS, et al (2014.) Targeting tumor suppressor networks for cancer therapeutics. *Curr Drug Targets*, **15**, 2-16.
- Horiuchi M, Iwanami J, Mogi M (2012). Regulation of angiotensin II receptors beyond the classical pathway. *Clin Sci*, **123**,193-203.
- Kong N, Zhang XM, Wang HT, et al (2013). Inhibition of growth and induction of differentiation of SMMC-7721 human hepatocellular carcinoma cells by oncostatin M. *Asian Pac J Cancer Prev*, **14**, 747-52.
- Liu Y, Zhang SF, Jin SM, et al (2003). Expression and location of a novel gene with cell differentiation in different tissues and cell lines. *Acta Laboratorium Animals Scientia Sinica*, **11**, 85-7.
- Li J, Meng FL, He LH, Zhang JZ (2012). Secreted protein HP1286 of *Helicobacter pylori* strain 26695 induces apoptosis of AGS cells. *Biomed Environ Sci*, **25**, 614-19.
- Liu M, Wu R, Yang F, et al (2013). Identification of FN1BP1 as a novel cell cycle regulator through modulating G1 checkpoint in human hepatocarcinoma hep3B cells. *PLoS One*, **8**, 57574.
- Niu JY, Liu J, Liu L, et al (2012). Construction of eukaryotic plasmid expressing human TGFBI and its influence on human corneal epithelial cells. *Int J Ophthalmol*, **5**, 38-44.
- Olin JL, Veverka A, Nuzum DS (2011). Risk of cancer associated with the use of angiotensin II-receptor blockers. *Am J Health Syst Pharm*, **68**, 2139-46.
- PylayevaGupta Y, Grabocka E, BarSagi D (2011). RAS oncogenes: weaving a tumorigenic web. *Nat Rev Cancer*, **11**, 761-74.
- Pappou EP, Ahuja N (2010). The role of oncogenes in gastrointestinal cancer. *Gastrointest Cancer Res*, **1**, 2-15.
- Herroo S, Beknal AK, Mahurkar N (2013). Immunomodulatory activity of methanolic extracts of fruits and bark of *Ficus glomerata* Roxb. In mice and on human neutrophils. *Indian J Pharmacol*, **45**, 130-35.
- Sankari SL, Masthan KM, Babu NA, Bhattacharjee T, Elumalai M (2012). Apoptosis in cancer--an update. *Asian Pac J Cancer Prev*, **13**, 7873-8.
- Tao HC, Wang HX, Dai M, et al (2013). Targeting SHCBP1 inhibits cell proliferation in human hepatocellular carcinoma cells. *Asian Pac J Cancer Prev*, **14**, 5645-50.
- Taylor Tavares AL, Willatt L, Armstrong R, et al (2013). Mosaic deletion of the NF1 gene in a patient with cognitive disability and dysmorphic features but without diagnostic features of NF1. *Am J Med Genet A*, **161**, 1185-8.
- Wei YY, Hou J, Tang WR, Luo Y (2012). The cooperation between p53 and Ras in tumorigenesis. *Yi Chuan*, **34**, 1513-21.
- Wang J, Lv XW, Du YG (2009). Potential mechanisms involved in ceramide-induced apoptosis in human colon cancer HT29 cells. *Biomed Environ Sci*, **22**, 76-85.
- Wang S, Wang Z (2013). Epigenetic aberrant methylation of tumor suppressor genes in small cell lung cancer. *J Thorac Dis*, **5**, 532-7.
- Yong Huang, Quan Zou, Sheng-peng Wang, et al (2011). Construction and detection of expression vectors of microRNA-9a in BmN cells. *J Zhejiang Univ Sci B*, **12**, 527-33.